Reports of Practical Oncology and Radiotherapy 25 (2020) 801–807

Available online at www.sciencedirect.com

Reports of Practical Oncology and Radiotherapy

journal homepage: http://www.elsevier.com/locate/rpor

Original research article

Efficiency of a novel non-monotonic segmented leaf sequence delivery of Varian MLC for non-split IMRT fields

Rose Kamal[a], Gaganpreet Singh[a], Deepak Thaper[a], Arun S. Oinam[b,*], Bhumika Handa[a], Vivek Kumar[a], Rakesh Kapoor[b]

[a] Centre for Medical Physics, Panjab University, Chandigarh, India
[b] Department of Radiotherapy, Post Graduate Institute of Medical Education and Research, Regional Cancer Centre, Chandigarh, India

ARTICLE INFO

Article history:
Received 15 April 2020
Received in revised form 7 June 2020
Accepted 27 July 2020
Available online 8 August 2020

Keywords:
NSLS algorithm
MU
MLC
NS
LMC
IMRT

ABSTRACT

Aim: Development of bidirectional non-monotonic segmented leaf sequence (NSLS) MLC delivery technique compatible with Varian MLC for non-split IMRT fields reducing total monitor units (TotalMU) and the number of segments (NS) simultaneously and assessment of its efficiency using a plan scoring index (PSI).

Materials and methods: The optimal fluence of IMRT plans of ten patients of lung carcinoma, calculated using Eclipse TPS version 11.0 (Varian Medical Systems, Palo Alto, CA, USA), was used to generate the segmented MLC fields using our newly developed equally spaced (ES) reducing level and NSLS algorithms in MATLAB® version 2011b for 6–10 intensity levels. These MLC fields were imported into the plans with the same field setup and the final dose was recalculated. The results were compared with those of commercially available multiple static segments (MSS) leaf motion calculation (LMC) algorithm and few previously published algorithms. Plan scoring index (PSI) and degree of modulation (DoM) was calculated to compare the quality of different plans for the same patient.

Results: The average differences in TotalMU and NS with respect to MSS algorithm are −3.80% and −14.28% for the NSLS algorithm, respectively. The calculated average PSI and DoM is 0.75, 2.51 and 0.91, 2.41 for the MSS and NSLS algorithms, respectively.

Conclusions: IMRT plans generated using the NSLS algorithm resulted in the best PSI, DoM values among all the leaf sequencing algorithms. Our proposed NSLS algorithm allows bidirectional delivery in Varian medical linear accelerator which is not commercially available. NSLS algorithm is efficient in reducing the TotalMU and NS with equivalent plan quality as that of MSS.

1. Background

Accurate dose delivery of intensity modulated radiation therapy (IMRT) depends upon the physical shape, size, and dosimetric properties of multileaf collimator (MLC) and the algorithm used for the calculation of leaf motion to realize the optimized fluence for the desired dose distribution.[1] Leaf sequencing (LS) algorithms for IMRT delivery determine the MLC positions of multiple segments as a function of monitor units (MU) to deliver the optimized fluence which is a matrix of $m \times n$ elements of non-negative integers. The LS algorithm plays an important role in the efficient treatment delivery of the desired optimized fluence in terms of total number of monitor units (TotalMU) and number of segments (NS). TotalMU affects the transmission, leakage radiation dose from collimator assembly as well as total body scatter dose.[2] NS affects the complexity of the treatment delivery and hence the wear and tear of MLCs. The dosimetric accuracy of treatment delivery has been also correlated with the complexity of the treatment plan. Various studies have been conducted to use modulation complexity of the treatment plan as a pre-treatment QA. Many authors suggested various complex modulation indices but degree of modulation (DoM) has been used as a measure of modulation complexity owing to its ease of use in routine clinics.[3,4]

IMRT treatments can be delivered in either step and shoot (segmental) or dynamic (sliding window) mode.[5] Various studies have been published for the scheming of LS algorithms to deliver dynamic and segmental treatments.[6,7] Dynamic delivery decreases the total treatment time at the expense of increased TotalMU. Que

* Corresponding author at: Department of Radiotherapy, Post Graduate Institute of Medical Education and Research, Regional Cancer Centre, Chandigarh 160012, India.
E-mail address: asoinam@yahoo.com (A.S. Oinam).

https://doi.org/10.1016/j.rpor.2020.07.005
1507-1367/

et al. reported that the sliding window algorithm results in more tongue-and-groove effect as compared to the reducing level segmental algorithm.[8] Yu et al. reported that the interplay effect for sliding window IMRT can result in variations greater than 100% of the desired intensity and is largely affected by beam width and speed of collimator motion.[9] Schaefer et al. also concluded that the magnitude of the interplay effect for step and shoot IMRT is negligible for thoracic tumors.[10] Verhey and Xia studied the ease of quality assurance of step and shoot over dynamic delivery.[11] The present study is mainly focused on step and shoot IMRT delivery technique in view of the aforesaid advantages.

In step and shoot IMRT delivery, MLCs move either unidirectionally in increasing step of positions or the bidirectional non-monotonic movement of leaf pairs. Siochi proposed a unidirectional leaf motion algorithm using rod pushing and extraction process on an intensity matrix that minimizes the MLC movement time for a given set of segments.[12] Medical linear accelerators of Varian Medical Systems of Palo Alto, CA, USA also provide a monotonically non-decreasing step function for leaf motion (unidirectional leaf motion) of MLC in both dynamic and step and shoot IMRT delivery.[13,14] However, the bidirectional motion of leaves reduces NS as compared to unidirectional segmentation.[15]

Bortfeld et al. devised a segmental algorithm that uses the fewest possible monitor units but is not heuristic for the minimization of NS, whereas reducing level algorithm proposed by Verhey and Xia decreases the number of segments at the cost of an increased number of monitor units.[11,16] The algorithm for a bidirectional step and shoot IMRT proposed by Engel results in minimum TotalMU and is heuristic for minimum NS.[17] Better performance of Engel's algorithm is also quoted over the well-established algorithm of Baatar et al. where both of these algorithms ensure optimal TotalMU, but Engel's algorithm results in lesser NS.[18] Still, the efficiency of the Engel leaf sequencing algorithm can be improved by removing very small segments.

In our study, the concept of minimum segment width was incorporated as an additional key constraint to the segmental LS algorithm of Konrad Engel.

2. Aim

The purpose of this study is to design the segmental leaf sequencing algorithm for non-monotonic MLC movements compatible with Varian linear accelerators to reduce TotalMU and NS. The results of the proposed algorithm are compared with various published algorithms for lung carcinoma cases.

3. Material and methods

The present study uses the optimal fluence generated in Eclipse treatment planning system (TPS) version 11.0 of Varian Medical Systems, Palo Alto, CA, USA for the development of a new LS algorithm. The new IMRT MLC fields are generated which are different from that of TPS generated MLC fields. The details of the workflow are given in the subsequent sections.

3.1. Patient selection

Ten patients with non-small cell lung carcinoma (NSCLC) were selected retrospectively for this study to demonstrate the efficiency of the proposed LS algorithm for non-split IMRT fields. 3D CT scans were acquired and population-specific ITV, PTV margins were given. Five field IMRT plans were made in Eclipse TPS using 6 MV beam with nominal dose rate of 300 MU/min for 40 Gy in 20 fractions (2 Gy/fraction). Dose volume optimization (DVO) algorithm version 11.0.31 was used for the optimization of IMRT plans followed by final dose calculation using anisotropic analytical algorithm (AAA) version 11.0.31 dose calculation algorithm. The plans were optimized with smoothing parameters of 50/30 for X/Y jaws incorporating inhomogeneity correction on the $2.5 \times 2.5\ mm^2$ dose calculation grid size. The plan acceptance criterion for planning target volume (PTV) was $V_{98\%} > 95\%$ and critical structures viz. bilateral lungs, heart, and spinal cord were spared according to the dose constraints recommended in QUANTEC.[19]

3.2. Processing of IMRT fluence

IMRT plans were generated using the DVO algorithm with multiple static segments (MSS) leaf motion calculation (LMC) algorithm available in Eclipse TPS for trilogy medical accelerator of Varian Medical Systems having millennium MLC (60 leaf pairs). The generated optimal fluence for each field was exported and processed using a new LS algorithm written in MATLAB® software version R2011b (The MathWorks, Natick, MA) which produces leaf sequence (.dva) files. The LS algorithm was designed in-house to minimize the TotalMU and NS simultaneously where the bidirectional movement of leaves for segmental delivery was allowed, referred to as non-monotonic segmented leaf sequence (NSLS) in the present study. Further, leaf sequences were also designed according to the criterion given by Verhey, Engel, Siochi and our newly developed equally spaced (ES) reducing level algorithms using a snippet of matRad.[20] The results of all the algorithms were compared with the proposed NSLS algorithm to check their efficiency. Each mlc (.dva) file generated from the in-house LS algorithm was verified using MLC shaper software (used for simulation and designing of mlc fields) of Varian Medical Systems and then imported into the new plan in Eclipse TPS with the same field parameters. The dose recalculation was performed using the same parameters as that of the original plan.

3.3. Leaf sequencing algorithms

The ES algorithm was designed using the concept of Verhey and Xia but the intensity map is divided into multiple segments of equal delivery intensity unit using a reducing level technique. The maximum and minimum value in the intensity matrix was used to determine the delivery intensity unit (d_k):

$$d_k = \frac{I_{max} - I_{min}}{l}, \quad (1)$$

where I_{max} is the maximum intensity value in fluence map, I_{min} is the minimum intensity value in a fluence map and l is the number of intensity levels (IL).

Considering each segment as a vector space (V) that can be piecewise discontinuous, the algorithm shapes the MLC leaves to a piecewise continuous area of the non-zero intensity of subspace of V that corresponds to one segment.

NSLS algorithm was developed using the concept of Engel leaf sequencing and the steps used to generate the segments for bidirectional NSLS algorithm are given below:

1. TPS generated 2D intensity profile (I of grid size $2.5\ mm \times 2.5\ mm$) was exported and processed using an in-house MATLAB program.
2. Centering of intensity fluence into 160×160 matrix corresponding to maximum field size ($40\ cm \times 40\ cm$).
3. Generation of segments (D_k) from 2D fluence using Engel's algorithm.
4. Each segment of the fluence matrix was rescaled to 60×160 according to the physical dimensions of Varian Millennium MLC configuration such that each row corresponds to one MLC leaf

pair (40 leaf pairs of 5 mm width and 20 leaf pairs of 10 mm width).
5. A key additional constraint of minimum segment width was incorporated to select the deliverable aperture segments which were different from those segments generated by Engel's algorithm. The algorithm calculates the area of each segment and the segments with an area greater than the user-defined threshold value ($\Delta A_{th} = 0.5\,cm^2$) were selected as deliverable segments. This constraint omits very small segments.
6. An offset was extracted from exported dva files of Eclipse generated plan and was applied to all the MLC leaf pairs to align the aperture of MLC field to the target volume.
7. MLC (.dva) file was written for Millennium 60 pair MLC in a Varian format.

The MLC file was written in Varian .dva file format as multiple segmented MLC fields, incorporating proper offset to all the MLC leaf pairs to align the aperture of the MLC field to the target volume. The cyclic redundancy check (CRC) information for the MLC file was generated while verifying the generated segmented leaf sequence with the MLC shaper. The verified MLC file was saved and imported into the new plan with the same field setup.

3.4. Comparison of treatment plans

Dose volume histograms (DVHs), TotalMU and NS of IMRT plans were calculated corresponding to 6–10 intensity levels for all the LMC algorithms as described in earlier sections. The plans were compared using several methods including slice by slice dose color wash, DVHs and plan quality metric based evaluation. In plan quality metrics, the conformity index (CI) and homogeneity index (HI), OAR doses, normalized TotalMU (MU_{norm}), normalized average number of segments (NS_{norm}), and DoM were used as parameters. A new plan scoring index (PSI) was also proposed to evaluate the relative plan quality and to compare the different plans generated for a patient using various algorithms.

DoM which is defined as the ratio of a total number of monitor units (Total MU) per fraction to dose per fraction in cGy as given in Eq. (2)[3,4]:

$$\mathrm{DoM} = \frac{\text{TotalMU per fraction}}{\text{Dose per fraction in cGy}}, \tag{2}$$

CI is defined as the ratio of the square of PTV covered by prescription isodose volume (PIV) to the product of PTV and PIV as defined in Eq. (3)[21]:

$$CI_p = \frac{PTV_{ref,p}^2}{PTV_p \times PIV_p}, \tag{3}$$

where $PTV_{ref,p}$ is volume of PTV covered by the prescription reference isodose curve for an arbitrary plan p, PTV_p is planning target volume and PIV_p is prescription isodose volume

HI is defined as follows[22]:

$$HI_p = \frac{D_{2\%} - D_{98\%}}{D_{50\%}}, \tag{4}$$

where $D_{2\%}$ is dose received by 2% volume of PTV, corresponds to the maximum dose, $D_{98\%}$ is dose received by 98% volume of PTV, corresponds to the minimum dose and $D_{50\%}$ is dose received by 50% volume of PTV, corresponds to the reference dose.

For any arbitrary treatment plan p, MU_{norm} and NS_{norm} are obtained after normalizing TotalMU, NS_{avg} to corresponding values of MSS generated plan and is defined as follows:

$$\mathrm{MU_{norm}} = \frac{(\mathrm{TotalMU})_p}{(\mathrm{TotalMU})_{MSS}}, \tag{5}$$

$$\mathrm{NS_{norm}} = \frac{(\mathrm{NS_{avg}})_p}{(\mathrm{NS_{avg}})_{MSS}}, \tag{6}$$

PSI_p is defined as follows:

$$\mathrm{PSI}_p = \frac{(1 - \mathrm{HI})_p \times \mathrm{CI}_p}{\mathrm{MU_{norm}} \times \mathrm{NS_{norm}}}, \tag{7}$$

This plan scoring index can be used as one of the important parameters for relative comparison of different treatment plans generated for the same patient. A higher value of PSI indicates a better overall plan in terms of efficient (MU_{norm} and NS_{norm}) and qualitative (CI, HI) treatment. The higher the values of MU_{norm} and NS_{norm}, the lower is its efficiency and PSI. One way ANOVA analysis was performed to test the statistical variation of CI, HI, DoM, OAR and PTV doses between various LS algorithms using SPSS v20.0.

4. Results

Fig. 1a–f represents the integrated fluence reconstructed from the stacking of multiple segmented MLC field of a typical fluence corresponding to seven intensity levels using ES, Engel, MSS,

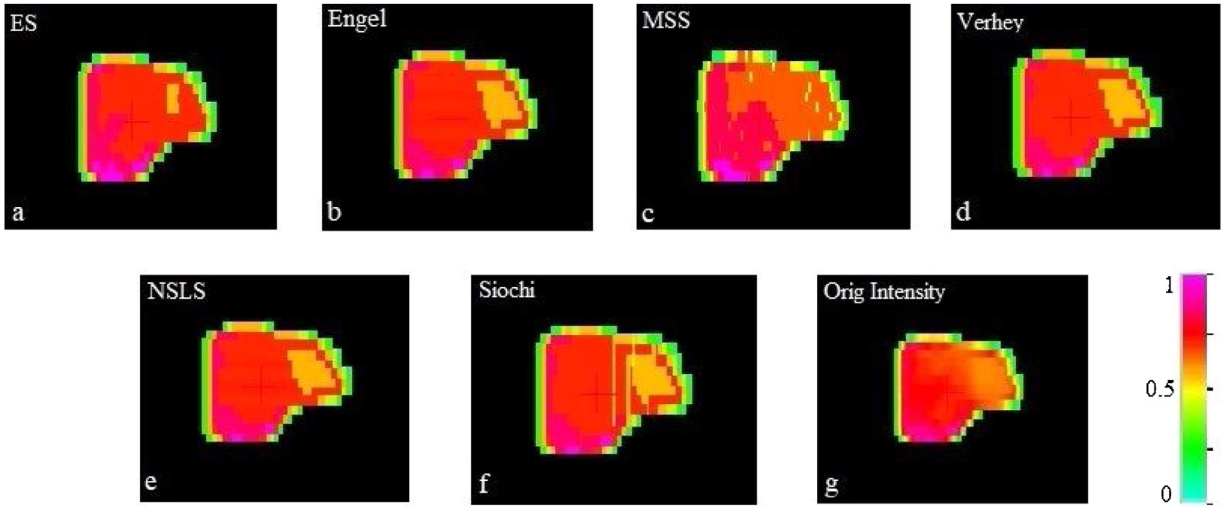

Fig. 1. Simulation of optical density profile in the MLC shaper software for a typical fluence (7 IL), of the different IMRT plans based on the (a) ES, (b) Engel, (c) MSS, (d) Verhey, (e) NSLS and (f) Siochi algorithms. Orig Intensity (g) represents the originally exported fluence.

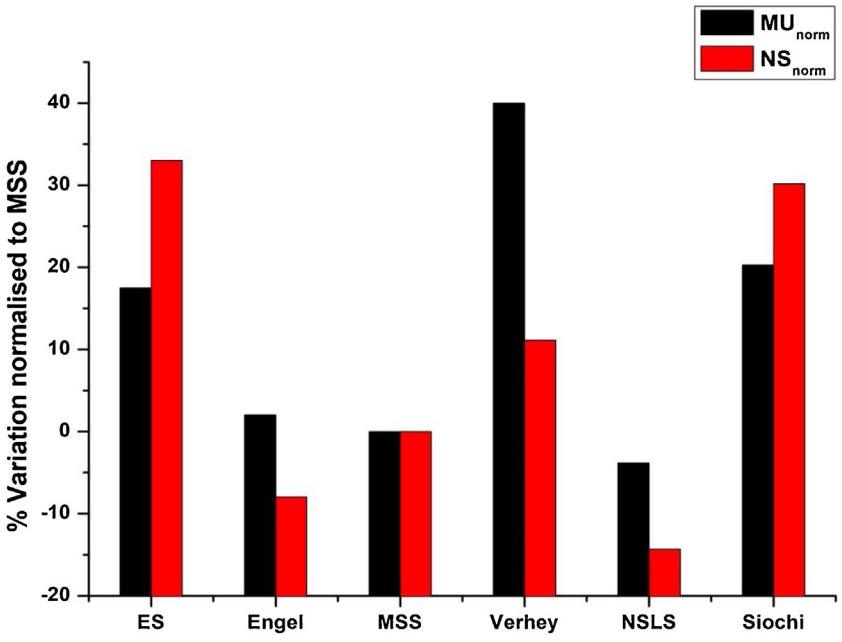

Fig. 2. Comparison of MU_{norm} and NS_{norm} of various leaf sequencing algorithms averaged over all cases.

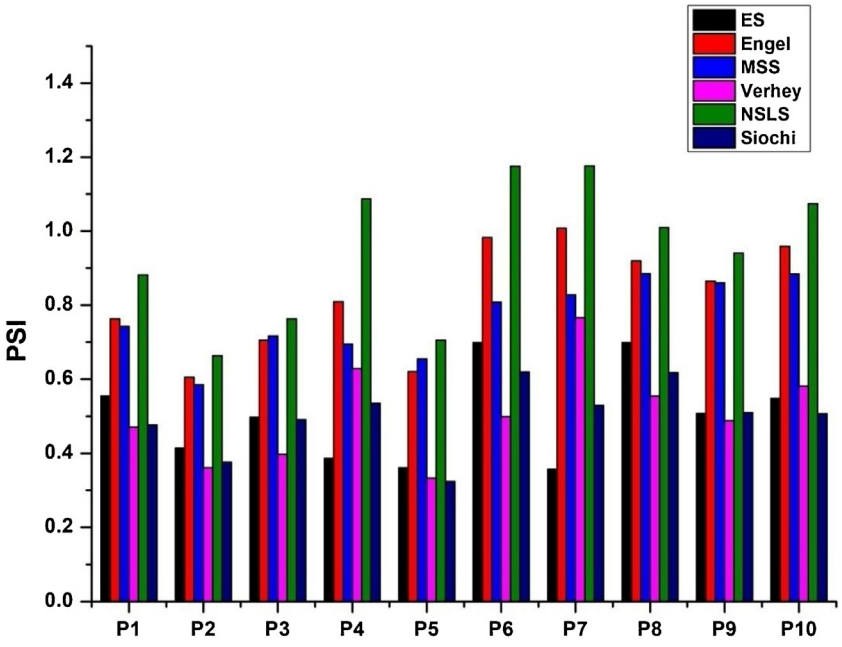

Fig. 3. Variation of PSI of all ten patients for all algorithms averaged over 6–10 IL.

Verhey, NSLS, and Siochi based leaf sequencing algorithms. The integrated fluence is simulated in MLC shaper software used for verification of segments. Fig. 1c and f shows the variation in integrated fluence which can be attributed to the inherent difference in both of these algorithms. MSS results in a unique solution for minimum MU for unidirectional MLC movement as it eliminates zero gradient points of fluence. This algorithm uses positive and negative gradient points of fluence and a number of discrete intensity levels to define the segments, whereas Siochi follows extraction and rod pushing process which may or may not be close to minimum MU. For the rest of the bidirectional techniques, the integrated fluence is comparable (Fig. 1a, b, d, and e). However, a subtle difference can be seen in the total fluence of ES (Fig. 1a) versus Verhey (Fig. 1d) which is due to the difference in the selection of delivery units for reducing the level technique. Fig. 1g represents the exported original optimal fluence of a typical field which is used as input data to generate the MLC fields of different leaf sequencing algorithms.

Fig. 2 represents the comparison of MU_{norm} and NS_{norm} averaged over all patients and IL (6–10) for each algorithm. As clearly seen, MU_{norm} and NS_{norm} are the lowest for the NSLS algorithm. The average change in TotalMU is 17.47%, 2.03%, 39.99%, −3.80%, 20.30% for ES, Engel, Verhey, NSLS, Siochi, respectively, with respect to the MSS algorithm, whereas average change in NS is 33.03%, −7.94%, 11.14%, −14.28%, 30.19% for ES, Engel, Verhey, NSLS, Siochi, respectively, with respect to the MSS algorithm.

Fig. 3 represents the variation of PSI for all the algorithms averaged over 6–10 ILs and PSI for the NSLS algorithm in each case is better than other algorithms. Fig. 4 represents the relative varia-

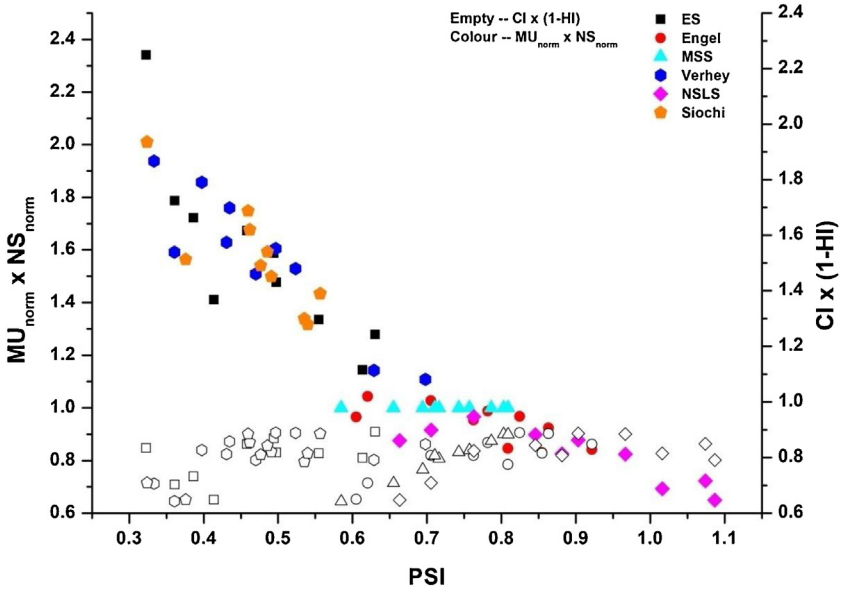

Fig. 4. Variation of PSI with $MU_{norm} \times NS_{norm}$ and $CI \times (1 - HI)$ for all patients and algorithms studied. Color filled markers depict the multiplication values of MU_{norm} and NS_{norm}, and Empty black markers represent the multiplication values of $(1 - HI)$ and CI.

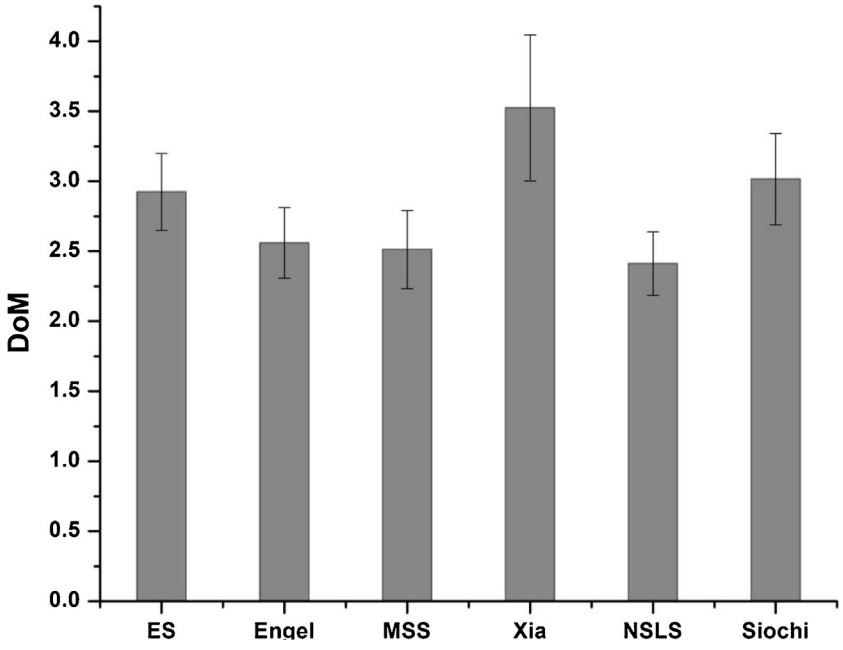

Fig. 5. Mean and standard deviation of DoM for all algorithms averaged over 6–10 IL of all ten patients.

tion of the factors used in the calculation of PSI. The multiplication factors affected by the denominator (MU_{norm}, NS_{norm}) and numerator (CI, (1-HI)) are plotted for all algorithms for all patients against PSI. From Fig. 4, it is clear that PSI calculations for all algorithms are largely affected by the denominator (product of MU_{norm} and NS_{norm}), as the numerator which is the product of CI and $(1 - HI)$ has comparable values. The data points corresponding to Verhey and Xia, Siochi and ES algorithms are clustered toward the lowest PSI value and correspond to a relatively higher value of denominator. PSI for MSS and Engel algorithms are clustered in the central region of the graph, whereas NSLS algorithm resulted in the PSI values in the range from 0.66 to 1.09 due to relatively lower values of denominator. Fig. 5 represents the variation of DoM for all the algorithms averaged over 6–10 ILs. The NSLS algorithm resulted in treatment plans with the lowest degree of modulation.

Table 1 represents the detailed comparison of critical organs and PTV doses obtained in treatment planning for 6–10 ILs corresponding to all the algorithms. The doses of these critical organs show that plans based on different algorithms are equivalent clinically ($p > 0.05$ using one way ANOVA).

5. Discussion

Few publications are available for the comparison of different leaf sequencing algorithms for clinical step and shoot IMRT plans. In this study, different aforementioned LS algorithms were used to generate the segments from exported fluence corresponding to 6–10 intensity levels. Thus, a total of 1500 multiple segmented fields are generated. However, there is no restriction in selecting

Table 1
Variations in PTV and OAR doses corresponding to average of 6–10 IL for various leaf sequencing algorithms.

Case	Parameter	Heart		Lungs		Cord	PTV
		V_{5Gy} (%)	D_{Mean} (Gy)	V_{20Gy} (%)	D_{Mean} (Gy)	D_{max} (Gy)	D_{Mean} (Gy)
Patient 1	Range	2.31	0.20	0.64	0.22	4.63	0.04
	Mean	14.31	2.26	11.85	8.05	23.56	39.40
	SD	0.50	0.05	0.16	0.06	1.16	0.01
Patient 2	Range	0.17	0.03	1.80	0.11	2.48	0.04
	Mean	0.29	0.85	7.51	6.02	9.38	41.16
	SD	0.04	0.01	0.42	0.03	0.63	0.01
Patient 3	Range	10.21	0.55	3.41	0.66	1.89	2.32
	Mean	40.65	5.55	11.14	7.72	8.80	41.48
	SD	2.47	0.20	0.80	0.12	0.54	0.43
Patient 4	Range	1.07	0.28	0.82	0.39	4.66	0.04
	Mean	11.08	1.41	3.92	3.65	14.70	40.84
	SD	0.32	0.08	0.19	0.09	1.14	0.01
Patient 5	Range	0.62	0.30	2.28	0.36	5.66	0.04
	Mean	19.40	4.43	11.01	8.44	21.58	40.64
	SD	0.17	0.07	0.42	0.09	1.08	0.01
Patient 6	Range	1.83	1.56	2.91	0.95	3.10	0.06
	Mean	53.87	9.03	11.77	8.03	15.96	42.16
	SD	0.45	0.28	0.68	0.16	0.75	0.02
Patient 7	Range	0.27	0.06	0.99	0.12	4.90	0.04
	Mean	4.82	1.13	11.18	6.96	16.83	40.48
	SD	0.08	0.02	0.20	0.03	1.32	0.01
Patient 8	Range	1.41	0.21	0.99	0.29	3.20	0.04
	Mean	13.96	2.49	11.47	8.27	19.91	40.76
	SD	0.30	0.04	0.22	0.07	0.79	0.01
Patient 9	Range	1.87	0.17	0.78	0.48	4.00	0.00
	Mean	7.66	1.84	16.78	8.63	27.79	40.00
	SD	0.43	0.04	0.19	0.11	0.95	0.00
Patient 10	Range	2.94	0.59	0.70	0.25	3.40	0.04
	Mean	42.29	6.91	17.98	9.89	23.32	40.64
	SD	0.62	0.14	0.17	0.08	0.85	0.01

the number of intensity levels whereas increasing the intensity levels to a higher extent may not significantly affect the plan quality but total treatment time will increase. The CI and HI are statistically comparable for 6–10 IL ($p > 0.05$ using one way ANOVA) in this study.

The step and shoot delivery have various advantages over dynamic delivery. The total treatment time is highly influenced by the number of segments in step and shoot IMRT. Engel developed a special algorithm for the minimization of TotalMU and NS simultaneously. At each step, an admissible duplet is selected such that the segments have the maximum potential for minimum MUs and are heuristic for minimum NS. In our work, an alternate method of IMRT delivery for non-split fields is proposed that incorporates a new constraint of minimum segment width of MLC into Engel leaf sequencing. NSLS is compared with both segmental bidirectional (Engel, Verhey, ES) and unidirectional algorithms (Siochi, MSS) in this study. Verhey and Xia proposed the reducing level algorithm using the concept of large segments opening which starts searching from the highest intensity level. The delivery intensity unit for each segment is selected in such a way that larger intensity levels are delivered initially and the deliverable units are recalculated from the residual intensity map to find the maximum intensity level again. Thus, the intensity values are reduced exponentially in subsequent segments until the lowest level of intensity is delivered and results in higher resolution of intensity split at the peak of fluence profile (because of unequal intensity split). Fig. 1a (ES) and d (Verhey) shows a difference in higher intensity areas and is attributed to the difference in resolution of intensity split at the peak of the fluence profile. Verhey's algorithm gives the maximum number of TotalMU because of small aperture openings corresponding to the peak of fluence profile.

Our ES algorithm, which is based on the idea of Verhey algorithm but with equal intensity split resolution over the fluence profile, results in a somewhat lower TotalMU than Verhey algorithm. The unequal intensity split (exponential) of Verhey's algorithm results in lesser deliverable units in contrast to ES that increases the number of segments in ES. Siochi's unidirectional algorithm results in drastic increase in NS. MSS and Engel give optimal TotalMU and NS simultaneously. But the NSLS algorithm provides minimum TotalMU and NS in comparison to all other algorithms and is attributed to the exclusion of tiny segments, which does not affect the dose distribution but increases TotalMU as well as AverageNS. The elimination of such small segments will be highly helpful to reduce dosimetric uncertainties due to motion effects. The calculated PSI indicates the efficiency of the NSLS algorithm over the other algorithms studied, with clinically insignificant variation in OAR and PTV doses ($p > 0.05$ using one way ANOVA).

The complexity of treatment is quantified using DoM which is proportional to total MU delivered per unit fractional dose. As TotalMU is proportional to the number of segments and its area, DoM also takes into account the effect of segments. DoM was minimum for the NSLS algorithm; however, there was a non-significant difference against MSS and Engel algorithm ($p > 0.05$). A detailed study could be performed to evaluate the effectiveness of various complexity metrics in estimating plan complexity for IMRT. NSLS algorithm is validated for non-split IMRT fields. The results of this study have shown that treatment plans generated with the NSLS algorithm have better efficiency for IMRT treatment plan delivery.

6. Conclusions

NSLS based delivery technique shows a potential for reduction of the TotalMU and NS. The average differences in TotalMU and NS with respect to the MSS algorithm are −3.80% and −14.28% for the NSLS algorithm, respectively. The calculated average PSI and DoM is 0.75 and 2.51 and 0.91 and 2.41 for the MSS and NSLS algorithms, respectively. Moreover, the NSLS algorithm offers a new delivery technique that is not available in the LMC algorithm of Varian Medical Systems. Our NSLS algorithm resulted in a higher PSI value in comparison to other algorithms proposed by Engel,

Verhey, Siochi, MSS and our newly developed ES algorithm. MLC interplay effect will be investigated in future works using the NSLS algorithm in comparison to commercially available unidirectional delivery while using 4D motion gated IMRT delivery. Comprehensive site-specific and algorithm-specific planning studies involving parameters such as various modulation complexity parameters etc. will be performed before quoting any conclusion regarding the dose conformality capabilities of the technique with respect to available delivery methods.

Conflict of interest

The matlab code is made available to readers on request. The authors declare that they have no conflict of interests that could have appeared to influence the work reported in this paper.

Financial disclosure

This work was partially supported by DST-PURSE Grant.

Acknowledgments

The authors are thankful to DST-PURSE for financial assiatance.

References

1. LoSasso T, Chui C, Ling CC. Physical and dosimetric aspects of a multileaf collimation system used in the dynamic mode for implementing intensity modulated radiotherapy. *Med Phys*. 1998;25(10):1919–1927.
2. Dai J, Que W. Simultaneous minimization of leaf travel distance and tongue-and-groove effect for segmental intensity-modulated radiation therapy. *Phys Med Biol*. 2004;49(23):5319–5331, http://dx.doi.org/10.1088/0031-9155/49/23/009.
3. Jodda A, Piotrowski T, Kruszyna-Mochalska M, Malicki J. Impact of different optimization strategies on the compatibility between planned and delivered doses during radiation therapy of cervical cancer. *Reports Pract Oncol Radiother*. 2020;25(3):412–421, http://dx.doi.org/10.1016/j.rpor.2020.03.027.
4. Hubley E, Pierce G. The influence of plan modulation on the interplay effect in VMAT liver SBRT treatments. *Phys Med*. 2017;40:115–121, http://dx.doi.org/10.1016/j.ejmp.2017.07.025.
5. Chen DZ, Luan S, Wang C. Coupled path planning, region optimization, and applications in intensity-modulated radiation therapy. *Algorithmica (New York)*. 2011;60(1):152–174, http://dx.doi.org/10.1007/s00453-009-9363-7.
6. Convery DJ, Rosenbloom ME. The generation of intensity-modulated fields for conformal radiotherapy by dynamic collimation. *Phys Med Biol*. 1992;37(6):1359–1374, http://dx.doi.org/10.1088/0031-9155/37/6/012.
7. Langer M, Thai V, Papiez L. Improved leaf sequencing reduces segments or monitor units needed to deliver IMRT using multileaf collimators. *Med Phys*. 2001;28(12):2450–2458, http://dx.doi.org/10.1118/1.1420392.
8. Que W, Kung J, Dai J. "Tongue-and-groove" effect in intensity modulated radiotherapy with static multileaf collimator fields. *Phys Med Biol*. 2004;49(3):399–405, http://dx.doi.org/10.1088/0031-9155/49/3/004.
9. Yu CX, Jaffray DA, Wong JW. The effects of intra-fraction organ motion on the delivery of dynamic intensity modulation. *Phys Med Biol*. 1998;43(1):91–104, http://dx.doi.org/10.1088/0031-9155/43/1/006.
10. Schaefer M, Münter MW, Thilmann C, et al. Influence of intra-fractional breathing movement in step-and-shoot IMRT. *Phys Med Biol*. 2004;49(12):14–19, http://dx.doi.org/10.1088/0031-9155/49/12/N03.
11. Verhey L, Xia P. Multileaf collimator leaf sequencing algorithm for intensity modulated beams with multiple static segments. *Med Phys*. 1998;25(8):1424–1434.
12. Siochi RAC. Minimizing static intensity modulation delivery time using an intensity solid paradigm. *Int J Radiat Oncol Biol Phys*. 1999;43(3):671–680, http://dx.doi.org/10.1016/S0360-3016(98)00430-1.
13. Spirou SV, Chui CS. Generation of arbitrary intensity profiles by dynamic jaws or multileaf collimators. *Med Phys*. 1994;21(7):1031–1041, http://dx.doi.org/10.1118/1.597345.
14. Rh WS. Eclipse algorithms reference guide eclipse. *Distribution*. 2010.
15. Dai J, Zhu Y. Minimizing the number of segments in a delivery sequence for intensity-modulated radiation therapy with a multileaf collimator. *Med Phys*. 2001;28(10):2113–2120, http://dx.doi.org/10.1118/1.1406518.
16. Bortfeld TR, Kahler DL, Waldron TJ, Boyer AL. X-ray field compensation with multileaf collimators. *Int J Radiat Oncol Biol Phys*. 1994;28(3):723–730, http://dx.doi.org/10.1016/0360-3016(94)90200-3.
17. Engel K. A new algorithm for optimal multileaf collimator field segmentation. *Discret Appl Math*. 2005;152(1–3):35–51, http://dx.doi.org/10.1016/j.dam.2004.10.007.
18. Ehrgott M, Hamacher HW, Nußbaum M. Decomposition of matrices and static multileaf collimators: a survey. *Optim Med*. 2007:25–46, http://dx.doi.org/10.1007/978-0-387-73299-2_2.
19. Bentzen SM, Constine LS, Deasy JO, et al. Quantitative Analyses of Normal Tissue Effects in the Clinic (QUANTEC): an introduction to the scientific issues. *Int J Radiat Oncol Biol Phys*. 2010;76(3 suppl):3–9, http://dx.doi.org/10.1016/j.ijrobp.2009.09.040.
20. Cisternas E, Mairani A, Ziegenhein P, Jäkel O, Bangert M, Nazionale C. *matRad – a multi-modality open source 3D treatment planning toolkit*; 2015:1608–1611, http://dx.doi.org/10.1007/978-3-319-19387-8.
21. Hospital C. *A simple scoring ratio to index the conformity of radiosurgical treatment plans*. 2000;93(suppl 3):219–222.
22. Menzel HG. The international commission on radiation units and measurements. *J ICRU*. 2010;10(2):1–35, http://dx.doi.org/10.1093/jicru/ndq025.